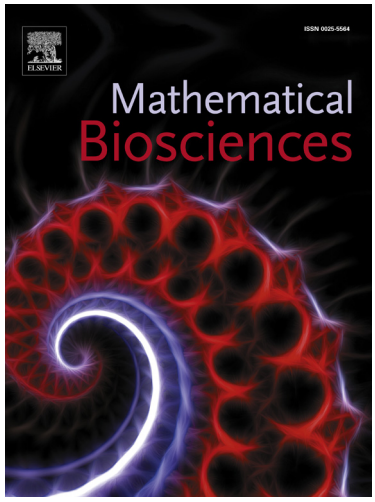

Identifying directional persistence in intracellular particle motion using Hidden Markov Models

Magnus Röding, Ming Guo, David A. Weitz, Mats Rudemo, Aila Särkkä

PII: S0025-5564(14)00002-9
DOI: http://dx.doi.org/10.1016/j.mbs.2013.12.008
Reference: MBS 7441

To appear in: *Mathematical Biosciences*

Please cite this article as: M. Röding, M. Guo, D.A. Weitz, M. Rudemo, A. Särkkä, Identifying directional persistence in intracellular particle motion using Hidden Markov Models, *Mathematical Biosciences* (2014), doi: http://dx.doi.org/10.1016/j.mbs.2013.12.008

Identifying directional persistence in intracellular particle motion using Hidden Markov Models

Magnus Röding(*)[a], Ming Guo[b], David A. Weitz[b], Mats Rudemo[a], Aila Särkkä[a]

[a] *Department of Mathematical Statistics, Chalmers University of Technology and Gothenburg University, Gothenburg, Sweden*
[b] *School of Engineering and Applied Sciences, Harvard University, Cambridge, MA, USA*

Abstract

Particle tracking is a widely used and promising technique for elucidating complex dynamics of the living cell. The cytoplasm is an active material, in which the kinetics of intracellular structures are highly heterogeneous. Tracer particles typically undergo a combination of random motion and various types of directed motion caused by the activity of molecular motors and other non-equilibrium processes. Random switching between more and less directional persistence of motion generally occurs.

We present a method for identifying states of motion with different directional persistence in individual particle trajectories. Our analysis is based on a multi-scale turning angle model to characterize motion locally, together with a Hidden Markov Model with two states representing different directional persistence. We define one of the states by the motion of particles in a reference data set where some active processes have been inhibited.

We illustrate the usefulness of the method by studying transport of vesicles along microtubules and transport of nanospheres activated by myosin. We study the results using mean square displacements, durations, and particle speeds within each state. We conclude that the method provides accurate identification of states of motion with different directional persistence, with very good agreement in terms of mean-squared displacement between the reference data set and one of the states in the two-state model.

Keywords: Particle tracking, Hidden Markov Models, transport processes, intracellular transport

(*) Corresponding author: Magnus Röding, Telephone: (+46) 31 772 49 92, E-mail: roding@chalmers.se, Address: Department of Mathematical Sciences, Chalmers University of Technology and Gothenburg University, 41296 Gothenburg, Sweden.

1. Introduction

The cytoplasm of eukaryotic cells is an out-of-equilibrium, network-like dynamic environment in which random forces collaborate with active processes on spatial organization, cell motility, import and export of materials, and internal transport [1]. ATP-consuming molecular motors are responsible for intracellular transport of large cargoes, such as large proteins, organelles, and vesicles [2, 3]. Random motion is a sufficiently effective means of transport of small molecules. However, larger structures rely on a more sophisticated infrastructure involving actin filaments, microtubules, and molecular motors, providing a range of options for different distances and particle sizes [4, 5, 6]. Indeed, it has been shown theoretically that rapid, random switching between random and a superposition of random and directed motion caused by e.g. binding and unbinding of motors is a 'search strategy' superior to pure random motion [7, 8]. Together with other types of motion such as anomalous diffusion, these dynamics of intracellular particles constitute the very core of the function of the cell including migration, division, deformation, and transport [9, 10, 11, 12, 13, 14, 2, 3]. In order to understand the function of the cell, it is vital to understand these transport processes.

Particle tracking is an increasingly popular technique for probing intracellular dynamics. Its appeal is the possibility to observe individual particles rather than just ensemble averages, thus providing richer information [15]. There is currently a great interest in developing new analysis methods to understand this type of data better. Many different approaches can be found in the existing literature i.e. fitting a Langevin-type evolution curve to experimental mean square displacement (MSD) data [4], time-resolved analysis based on local MSD and trajectory asymmetry to identify states of random, constrained, directed, and stalled motion [16], and separation of bursts of directed motion along microtubules from random motion based on thresholding of local MSD and a measure of local directional persistence [17]. See also [18] and references therein.

In this paper, we present a statistical method for identifying states of motion with different directional persistence in individual trajectories, for example inside the living cell. We employ a model for turning angles in several different time scales to characterize the degree of local directionality in every point along the trajectory. We assume that the particle trajectories exhibit random switching between two states, characterized by different directional persistence. We base our analysis on a Hidden Markov Model (HMM) [20, 21, 22], a statistical framework for modeling random switching dynamics where the switching as such is not observed but only its impact on the character of the particle trajectories. We define one of the states by the motion of particles in a reference data set where some active processes have been inhibited. We illustrate the usefulness of the method by studying transport of vesicles along microtubules and transport of nanospheres activated by myosin.

2. Materials and methods

2.1. A multi-scale model for directionality

The motion of individual particles in a cell is generally a superposition of thermal motion in a complex, viscoelastic medium and non-thermal motion, the precise nature of which is rarely if ever known. It would be a notoriously difficult task to formulate a comprehensive model of the dynamics of a tracer particle, even if no switching behavior is present. However, it is not our aim to provide a generative model but rather a simple model for quantification of directionality which captures the essence of the behavior.

We base our analysis on turning angles, used previously in e.g. [19] for particle tracking analysis. We define the turning angle to be simply the smallest angle between one trajectory increment and the next. Thus, straight forward means turning angle 0, straight to the side (making no distinction between left and right) means turning angle $\pi/2$, and straight backward means turning angle π. Although we here consider only 2D trajectories, a similar definition of turning angle is feasible in 3D as well.

To make the model more general and flexible, we consider several different time scales, all multiples of the shortest time scale Δt determined by the experimental time lapse between consecutive video frames. Thus, we measure n angles (in n time scales) at every point along a particle trajectory, represented by a vector in the hypercube $[0, \pi]^n$. Each state in the Hidden Markov Model (HMM) is then determined by a probability distribution over $[0, \pi]^n$ for the observations, i.e. all turning angles at all time scales are simultaneously used within the same model. However, since this distribution generally has a complex structure, we introduce a binary approximation, where 0 means forward (turning angle between 0 and $\pi/2$) and 1 means backward (turning angle between $\pi/2$ and π). By this simplification, the number of parameters in the HMM will be manageable. The local directionality is hence described by a value in $\{0, 1\}^n$, and each state (each 'type' of motion) corresponds to a probability distribution over this set of values for the observations.

The choice of time scales is a trade-off between temporal 'locality', identifiability of directional persistence, and the number of parameters in the model. In our investigation we have used the time scales Δt, $2\Delta t$, $3\Delta t$, $4\Delta t$, and $5\Delta t$, hence $n = 5$, see Fig. 1 for an illustration. However, there is room for some tweaking by choosing other multiples of Δt. It is worth noting that dependencies are introduced between the turning angle distributions at adjacent points. Therefore, the independence assumption in the HMM is only an approximation. It should also be noted that the value of Δt, selected in the course of the experiment, must be sensible with regard to the characteristic time scales of particle motion in the particular studied setting.

2.2. Hidden Markov Models

After having been introduced in the late 1960s and the early 1970s, Hidden Markov Models (HMMs) [20, 21, 22] have grown popular in a wide range of

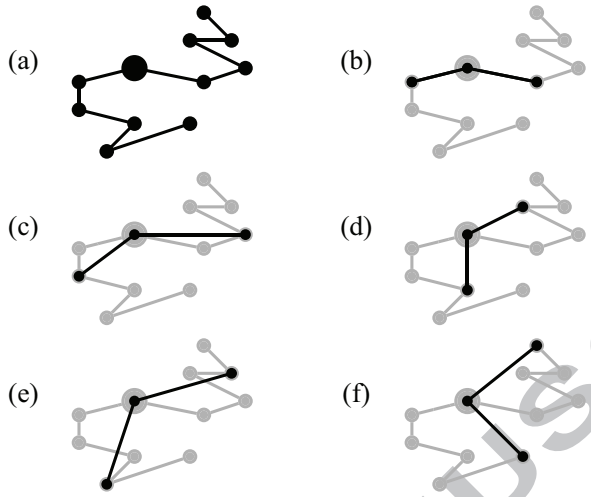

Figure 1: Illustration of the extraction of turning angles at different time scales around an arbitrary point (marked with an extra large spot) in a trajectory. From (a) an example trajectory, we illustrate how the turning angles are computed at time scales (b) Δt, (c) $2\Delta t$, (d) $3\Delta t$, (e) $4\Delta t$, and (f) $5\Delta t$. The turning angles range from 0 (straight forward), through $\pi/2$ (straight to the side, with no distinction between left and right) to π (straight backward). In this example, all turning angles are smaller than $\pi/2$ except at the $5\Delta t$ scale, so the corresponding, discretized binary turning angle vector would be $(0, 0, 0, 0, 1)$.

fields. The key idea is to model a sequence of observations depending on a corresponding unobserved (hidden) Markov chain, with a number of (hidden) states between which random switching occurs. HMMs have been used previously to model particle tracking data [23].

We assume that we have a (discrete-time) Markov chain with random switching between two states, corresponding to two different particle motions with different directional persistence. For a trajectory of length T (particle position recorded in T consecutive frames), this generates a state sequence $S = s_1 s_2 ... s_T$, for example '1122221112111...'. The state sequence S is (stationary) Markov i.e. the current state is only dependent on the previous state, so that

$$\begin{aligned} P(s_t = i_t | s_{t-1} = i_{t-1}, s_{t-2} = i_{t-2}, ...) \quad &= \\ P(s_t = i_t | s_{t-1} = i_{t-1}) \end{aligned} \tag{1}$$

for all t i.e. the probability that the chain is in a particular state i_t at time t only depends on the state i_{t-1} at time $t-1$. The random switching is quantified by the transition probabilities a_{ij} where

$$a_{ij} = P(s_t = j | s_{t-1} = i) \tag{2}$$

for all t and $i = 1, 2$ and $j = 1, 2$. We call the matrix $A = \{a_{ij}\}$ the transition matrix. The proportion of time spent in each state, π_1 and π_2, can be de-

rived assuming reversibility and the detailed balance condition $\pi_1 a_{12} = \pi_2 a_{21}$, yielding

$$\pi_1 = \frac{a_{21}}{a_{12} + a_{21}} \text{ and } \pi_2 = \frac{a_{12}}{a_{12} + a_{21}}. \tag{3}$$

In our case, the motion of the particle is observed, not the state sequence. In the HMM, we consider this motion a random outcome from the probability distribution of directions of the current state (known as the emission distribution of the state). Recall that the directions follow a probability distribution over $\{0,1\}^n$, where n is the number of time scales. Assume that for the state sequence S, we have a corresponding observation sequence $Q = q_1 q_2, ..., q_T$. Let

$$\theta_j(k) = P(q_t = k | s_t = j) \tag{4}$$

for all t and $k \in \{0,1\}^n$ be the probability that we observe value k given that the current state is j. Denote the two direction distributions for the two states by $\theta^{(1)}$ and $\theta^{(2)}$. We can now compute the joint probability of a particular state sequence and observation sequence given the transition matrix A and the emission distributions $\theta^{(1)}$ and $\theta^{(2)}$,

$$\begin{aligned} P(Q, S | A, \theta^{(1)}, \theta^{(2)}) = P(Q|S; \theta^{(1)}, \theta^{(2)}) P(S|A) \quad = \\ \theta_{s_1}(q_1) ... \theta_{s_T}(q_T) \pi_{s_1} a_{s_1 s_2} ... a_{s_{T-1} s_T}. \end{aligned} \tag{5}$$

Interpreting $P(Q, S|A, \theta^{(1)}, \theta^{(2)})$ as a function of its parameters for a fixed sequence of states and observations, this is the complete-data likelihood. However, since we do not observe the state sequence, we wish to compute the probability of the observations only, given the parameters, i.e. $P(Q|A, \theta^{(1)}, \theta^{(2)})$. This is obtained by summation of the joint probability $P(Q, S|A, \theta^{(1)}, \theta^{(2)})$ over all possible state sequences,

$$P(Q|A, \theta^{(1)}, \theta^{(2)}) = \sum_{S \in \{1,2\}^T} P(Q|S; \theta^{(1)}, \theta^{(2)}) P(S|A). \tag{6}$$

Interpreting $P(Q|A, \theta^{(1)}, \theta^{(2)})$ as a function of its parameters for a fixed sequence of observations, this is the incomplete-data likelihood $\mathcal{L}(A, \theta^{(1)}, \theta^{(2)}|Q)$, from which maximum likelihood estimates of the transition matrix and the emission distributions can be obtained. However, the number of terms in this sum grows exponentially in T, and directly maximizing the likelihood is infeasible in practice. Fortunately, iterative maximization of the likelihood can be done using the forward-backward (Baum-Welch) algorithm [21]. Once parameter estimates are obtained, one can find the most likely state for each time t in the sequence and hence effectively segmenting the trajectory into states of different directional persistence. Generalizing the HMM estimation scheme to several sequences (several trajectories) is straightforward.

The traditional HMM inference scheme focuses on the case where all observations are 'unlabeled', i.e. when the corresponding hidden state is unknown. However, a key idea in our approach is to provide an algorithm with information

on the characteristics of one of the two types of motion using data from a reference data set where some active processes have been inhibited. We can regard those data as the outcome of a 'degenerate' HMM where the state sequence is '111...1'. Thereby, we can estimate the probability distribution of directions (the emission distribution) of state 1 from those data just by computing the frequencies of observations for each value in $\{0,1\}^n$. These estimates $\hat{\theta}^{(1)}$ can then be incorporated into the HMM machinery by replacing the likelihood with a reduced likelihood $\mathcal{L}_{\text{reduced}}(A, \theta^{(2)}|Q) = P(Q|A, \hat{\theta}^{(1)}, \theta^{(2)})$, now a function of only A and $\theta^{(2)}$.

2.3. Particle tracking experiments

Two types of activation is studied experimentally, transport along microtubules and myosin-induced transport. In both cases, experimental observation is performed in A7 cells [24] cultured in DMEM with 2% fetal calf serum, 8% newborn calf serum (Invitrogen, Merelbeke, Belgium), 10 mM HEPES buffer, and 100 unit/ml PenStrep at 37°C and 5% CO_2. MatTek dishes with No. 1 glass coverslip as the bottom are coated with 0.1 mg/ml collagen I for 2 h at 37°C. The cells are then plated on dishes at 20 cells/mm^2 over night.

For studying transport along microtubules, vesicles are tracked. Vesicles are sub-micron spherical objects in the cell that bud off from cellular membranes to form sub-micron-scale carriers that facilitate intracellular transport of materials. In our experiment, vesicles are directly imaged with bright-field microscopy using excitation from a 633 nm laser and a 63x/1.2NA water immersion lens on a Leica TSC SP5 microscope. These vesicles are occasionally transported by molecular motors along microtubule tracks. To inhibit this directional transport in order to produce a reference data set, 10 μM nocodazole (Sigma-Aldrich, Corvallis, MO), a chemical interfering with the polymerization of microtubules, is added to cell media for 4 h incubation. The trajectories are recorded with time lag $\Delta t = 0.107$ s and pixel size $\Delta x = 0.096$ μm.

For studying myosin-activated motion, polystyrene nanospheres are tracked. Yellow-green fluorescent carboxylate-modified polystyrene nanospheres of nominal size 200 nm (Molecular Probes, Invitrogen, Merelbeke, Belgium) are rendered inert [25] by immersion in a 1 mg/ml PEG (4 kDa) conjugated poly-L-lysine solution (Surface Solutions, Dübendorf, Switzerland) for 1 h at room temperature, then washed twice with PBS, stored at 4°C, and used within 48 hours. The particles are diluted to a final concentration of 10^7 part/ml in PBS and injected into the cells by using a glass needle and a FemtoJet microinjector (Eppendorf, Hamburg, Germany) mounted on a microscope. Each cell is only injected with up to 50 particles to reduce the interference to cell function. Cells are allowed to recover in culture medium for 6 h and are then imaged in culture media at 37°C and 5% CO_2 on a confocal microscope using excitation from the 488 nm line of an argon laser and a 63x/1.2NA water immersion lens on a Leica TSC SP5 microscope. To inhibit the contracting activity generated by myosin II motors in order to produce a reference data set, blebbistatin (Toronto Research Chemicals, Toronto, Canada), a specific inhibitor that keeps myosin

II in a weakly bound state to actin [26] is dissolved in DMSO and added to cell media to a 10 μM final concentration for 30 min incubation. The trajectories are recorded with time lag $\Delta t = 0.07$ s and pixel size $\Delta x = 0.08$ μm.

At least 50 cells were assessed over many independent experiments for both the transport along microtubules and the myosin-activated motion and for both wild type cells and cells treated with inhibitors. The images are processed with particle tracking software written by J. Crocker, D. Grier and E. Weeks (http://www.physics.emory.edu/∼weeks/idl/).

3. Results

We evaluate the method by studying transport along microtubules and myosin-activated motion. First, the emission distribution of one of the states is estimated from the reference data sets where activity has been inhibited by addition of nocodazole and blebbistatin, respectively. Second, the Baum-Welch algorithm for inference in the HMM is run with one of the emission distributions fixed. A large number of runs is performed in parallel to ensure convergence to the maximum likelihood parameter estimates, and the most likely state sequences are estimated. The result is a separation of the trajectories into 'active' parts and 'not active' parts. It is important to point out that 'not active' in this case refers to a specific type of activation being inhibited, whereas other types of activation may still be present. In order to understand the nature of the particle motion and the separation into different states, we consider several parameters such as mean-squared displacement (MSD), duration of states and particle speed. MSD plots are powerful tools to study the nature of motion. In Fig. 2, we compare the MSD of the two identified states with the MSD of the reference (inhibited) data sets. The reference data sets correspond to the 'not active' state, and the slopes of the corresponding MSDs indicate approximately Brownian behavior. As can be seen, the 'not active' state of the wild type data shows very good agreement with the MSD of the reference data sets over all time scales shown, suggesting a good identification of the specific modeled activity. The fact that the agreement holds for time scales much longer than the time scales included in the multi-scale directionality model indicates that those time scales provide sufficient information to capture the essential behavior of the specific activated motion. In Fig. 3, histograms of the durations of different states are shown. For both data sets, substantially more time is spent in the 'not active' state, see also Tab. 1, the activations generally being short bursts. In Fig. 4, histograms of speeds evaluated at a characteristic time scale equal to the multiple of Δt closest to the average duration of the 'active' state are shown. The difference in average speed is substantial between the states, about a factor of 3 as can also be seen in Tab. 1. We also study example trajectories from both data sets. In Fig. 5, an example trajectory for transport along microtubules is shown. Turning angles, discretized turning angles, the sequence of probabilities of states and the identified most likely states are shown together with the segmented trajectory itself. In Fig. 6, the same is shown for

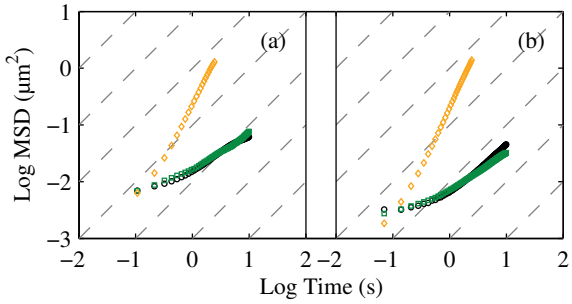

Figure 2: Mean squared displacements (MSDs) for (a) transport along microtubules and (b) myosin-activated motion. Trajectories of particles in wild type cells are separated into an 'active' state (yellow, diamonds) and a 'not active' state (green, squares). The 'not active' state shows very good agreement with the MSD of the reference (inhibited) data sets (black, circles) over all time scales shown, suggesting a good identification of the specific modeled activity. Slopes equal to 1 are indicated by dashed lines.

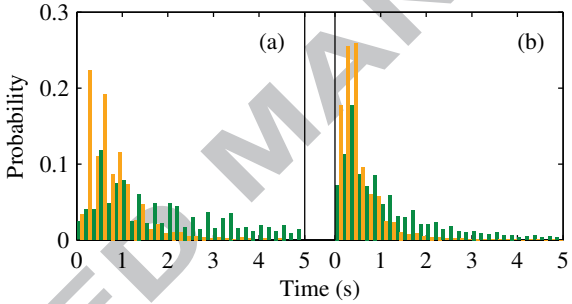

Figure 3: Histogram of durations of different states for (a) transport along microtubules and (b) myosin-activated motion. Trajectories of particles in wild type cells are separated into an 'active' state (yellow) and a 'not active' state (green).

Table 1: Results

	Microtubules		Myosin	
	Not active	Active	Not active	Active
Time spent in state (%)	81.79	18.21	76.40	23.60
Mean duration (s)	3.2997	0.7830	1.6136	0.5082
Mean speed (μm/s)	0.1114	0.3733	0.1086	0.3254

the myosin-activated motion. The method here delivers a plausible identification of active bursts, and we see clearly that there is switching between slower and longer 'not active' transport and faster and shorter 'active' transport, in

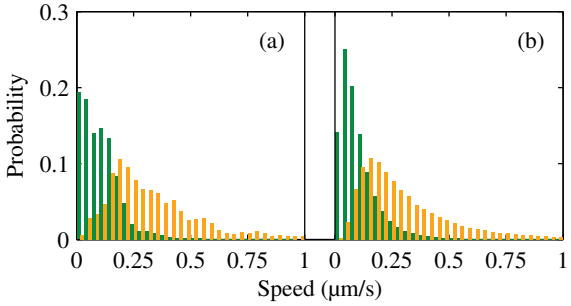

Figure 4: Histogram of speeds in different states for (a) transport along microtubules and (b) myosin-activated motion. Trajectories of particles in wild type cells are separated into an 'active' state (yellow) and a 'not active' state (green). The speeds are measured at a characteristic time scale equal to the multiple of Δt closest to the average duration of the 'active' state.

agreement with what Figs. 3 and 4 indicates.

4. Discussion and conclusion

We have presented a method for identifying directional persistence in intracellular particle motion using Hidden Markov Models (HMMs). Trajectories of tracer particles are segmented by identifying states of different directional persistence, using a model for turning angles in several time scales to characterize and quantify motion and the degree of directionality locally in every point along the trajectory. We assume that the particle trajectories exhibit random switching between two states, where the turning angle distribution of one of the states is estimated from reference data sets where activity has been inhibited. This prior 'calibration' to a specific type of activation/inhibited activation is one of the key points of the method. The reason is that arbitrary cutoffs to define different types of motion, such as threshold values, can be avoided. The method should be of interest in all cases where activation leads to increased directional persistence.

We illustrate the usefulness of the method by transport of vesicles along microtubules and myosin-activated motion of nanospheres. The resulting mean square displacements, durations, and particle speeds within each state indicate a good separation into 'active' and 'not active' states which is consistent with the characteristics of 'not active' as determined from reference data sets with inhibited activation.

Regarding future work, the binary turning angle distribution used to quantify directionality is quite crude and could be improved. The reason for introducing the binary approximation, taking into account only forward and backward turns, was mainly to keep the number of parameters in the model low. Ideally, using conceptually the same model, one would want to model a continuous

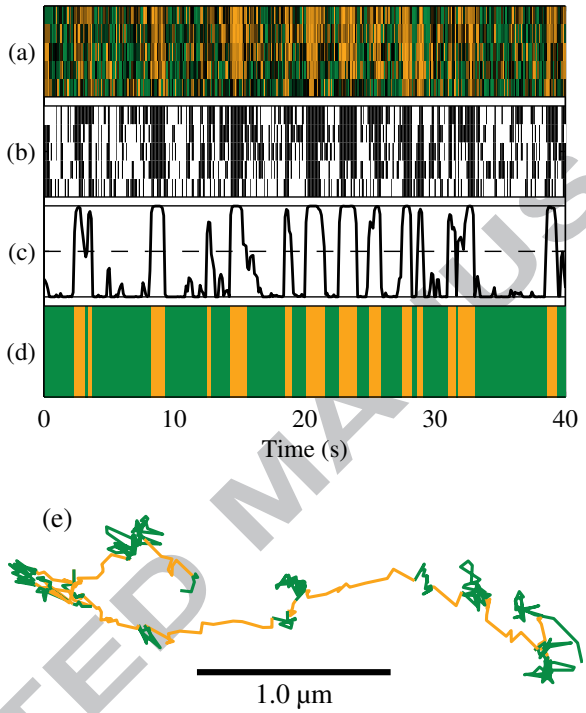

Figure 5: An illustrative trajectory segment for transport along microtubules studied over a 40 s range. In (a), the turning angles at five different time scales (from bottom to top 0.07 s, 0.14 s, 0.21 s, 0.28 s, 0.35 s), where the color map goes from green (straight backward) through black (straight to the side) to yellow (straight forward), are shown. In (b), the corresponding discretized turning angles with forward (black) and backward (white) are shown. In (c), the probability sequence that is thresholded at 0.5 to yield a segmentation of the trajectory into 'active' and 'not active' states is shown. In (d), the identified 'active' (yellow) and 'not active' (green) states are shown. In (e), the segmented trajectory itself is shown.

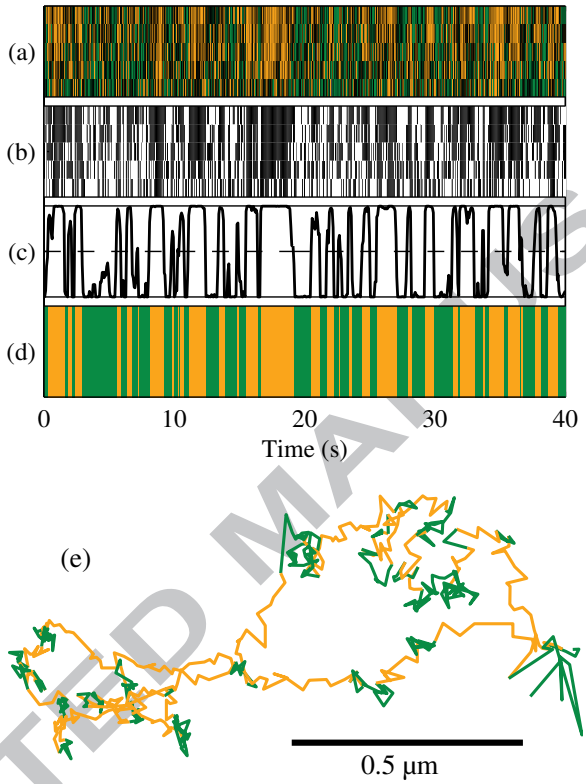

Figure 6: An illustrative trajectory segment for myosin-activated motion studied over a 40 s range. In (a), the turning angles at five different time scales (from bottom to top 0.07 s, 0.14 s, 0.21 s, 0.28 s, 0.35 s), where the color map goes from green (straight backward) through black (straight to the side) to yellow (straight forward), are shown. In (b), the corresponding discretized turning angles with forward (black) and backward (white) are shown. In (c), the probability sequence that is thresholded at 0.5 to yield a segmentation of the trajectory into 'active' and 'not active' states is shown. In (d), the identified 'active' (yellow) and 'not active' (green) states are shown. In (e), the segmented trajectory itself is shown.

distribution of turning angles, effectively estimating a conditional probability distribution over the hypercube $[0, \pi]^n$ for each state. However, attempts to do this indicated that the number of parameters in the model grows too large for feasible inference. The 5 time scales selected is a trade-off both in terms of the number of selected scales, and which scales are selected. On the one hand, an analysis which is as 'localized' as possible is appealing. On the other hand, a single point along a trajectory contains no information, so by necessity, some 'rolling-window' approach is inevitable. How to 'optimally' select time scales remains an open question, although the validity of a selection can be empirically studied as shown herein. This approach introduces some dependencies between consecutive observations in the HMM that could be accounted for in further development of the method. Generalizations of the HMM e.g. the hierarchical Hidden Markov Model or the Hidden semi-Markov Model could be used to generalize the model but would substantially increase the complexity.

In conclusion, using particle tracking to study how thermal and non-thermal forces collaborate in the cell remains an important research topic for gaining understanding on spatial organization, cell motility, import and export of materials, and internal transport. This new proposed framework for particle tracking data analysis of activation, with calibration using a data set without activation, shows promise for further investigations on the nature of intracellular motility.

5. Acknowledgments

We thank Vasily Zaburdaev for useful discussions. Some of the computations were performed on C3SE (Chalmers Centre for Computational Science and Engineering) computing resources. SuMo Biomaterials is acknowledged. This work has been carried out with financial support from the Swedish Foundation for Strategic Research (SSF) through Gothenburg Mathematical Modelling Center (GMMC), from the foundations Stiftelsen Olle Engkvist Byggmästare, Längmanska Kulturfonden, Wilhelm och Martina Lundgrens Vetenskaps- och Understödsfonder, Chalmers Vänner, the BIOSUM research school, and the Harvard Materials Research Science and Engineering Center (DMR-0820484).

References

[1] C. Brangwynne, G. Koenderink, F. MacKintosh, D. Weitz, Cytoplasmic diffusion: molecular motors mix it up, J Cell Biol 183 (2008) 583–587.

[2] A. Caspi, R. Granek, M. Elbaum, Enhanced diffusion in active intracellular transport, Phys Rev Lett 85 (2000) 5655–5658.

[3] A. Caspi, R. Granek, M. Elbaum, Diffusion and directed motion in cellular transport, Phys Rev E 66 (2002) 1–12.

[4] J. Snider, F. Lin, N. Zahedi, V. Rodionov, C. Yu, S. Gross, Intracellular actin-based transport: How far you go depends on how often you switch, PNAS 101 (2004) 13204–13209.

[5] S. Gross, M. Tuma, S. Deacon, A. Serpinskaya, A. Reilein, V. Gelfand, Interactions and regulation of molecular motors in Xenopus melanophores, J Cell Biol 156 (2002) 855–865.

[6] V. Rodionov, J. Yi, A. Kashina, A. Oladipo, S. Gross, Switching between microtubule- and actin-based transport systems in melanophores is controlled by cAMP levels, Curr Biol 13 (2003) 1837–1847.

[7] C. Loverdo, O. Bénichou, M. Moreau, R. Voituriez, Enhanced reaction kinetics in biological cells, Nature Phys 4 (2008) 134–137.

[8] S. Klumpp, R. Lipowsky, Active diffusion of motor particles, Phys Rev Lett 95 (2005) 268102.

[9] C. Parent, P. Devroutes, A cell's sense of direction, Science 284 (1999) 765–770.

[10] R. Insall, A. Müller-Taubenberger, L. Machesky, J. Kähler, E. Simmeth, S. Atkinson, I. Weber, G. Gerisch, Dynamics of the Dictyostelium Arp2/3 complex in endocytosis, cytokinesis, and chemotaxis, Cell Motil Cytoskeleton 50 (2001) 115–128.

[11] C. Konopka, J. Schleede, A. Skop, S. Bednarek, Dynamin and cytokinesis, Traffic 7 (2006) 239–247.

[12] D. Fletcher, R. Mullins, Cell mechanics and the cytoskeleton, Nature 463 (2010) 485–492.

[13] P. Hänggi, F. Marchesoni, Artificial Brownian motors: controlling transport on the nanoscale, Rev Mod Phys 81 (2009) 387–442.

[14] M. Otten, A. Nandi, D. Arcizet, M. Gorelashvili, B. Lindner, D. Heinrich, Local motion analysis reveals impact of the dynamic cytoskeleton on intracellular subdiffusion, Biophys J 102 (2012) 758–767.

[15] V. Levi, E. Gratton, Exploring dynamics in living cells by tracking single particles, Cell Biochem Biophys 48 (2007) 1–15.

[16] S. Huet, E. Karatekin, V. Tran, I. F. S. Cribier, J.-P. Henry, Analysis of transient behavior in complex trajectories: application to secretory vesicle dynamics, Biophys J 91 (2006) 3542–3559.

[17] D. Arcizet, B. Meier, E. Sackmann, J. Rädler, D. Heinrich, Temporal analysis of active and passive transport in living cells, Phys Rev Lett 101 (2008) 248103.

[18] N. Gal, D. Lechtman-Goldstein, D. Weihs, Particle tracking in living cells: a review of the mean square displacement method and beyond, Rheol Acta 52 (2013) 1–19.

[19] C. Pallavicini, M. Despósito, V. Levi, L. Bruno, Analysis of persistence during intracellular actin-based transport mediated by molecular motors, Journal of Physics: Conference Series 246 (2012) 012038.

[20] L. E. Baum, T. Petrie, Statistical inference for probabilistic functions of finite state Markov chains, Ann Math Stat 37 (1966) 1554–1563.

[21] L. E. Baum, T. Petrie, G. Soules, N. Weiss, A maximization technique occurring in the statistical analysis of probabilistic functions of Markov chains, Ann Math Stat 41 (1970) 164–171.

[22] L. E. Baum, An equality and associated maximization technique in statistical estimation of probabilistic functions of Markov processes, Inequalities 3 (1972) 1–8.

[23] R. Das, C. Cairo, D. Coombs, A Hidden Markov Model for single particle tracks quantifies dynamic interactions between LFA-1 and the actin cytoskeleton, PLoS Comp Biol 5 (2009) e1000556.

[24] C. Cunningham, J. Gorlin, D. Kwiatkowski, J. Hartwig, P. Janmey, H. Byers, T. Stossel, Actin-binding protein requirement for cortical stability and efficient locomotion, Science 255 (1992) 325–327.

[25] M. Valentine, Z. Perlman, M. Gardel, J. Shin, P. Matsudaira, T. Mitchison, D. Weitz, Colloid surface chemistry critically affects multiple particle tracking measurements of biomaterials, Biophys J 86 (2004) 4004–4014.

[26] A. Straight, A. Cheung, J. Limouze, I. Chen, N. Westwood, J. Sellers, T. Mitchison, Dissecting temporal and spatial control of cytokinesis with a myosin II inhibitor, Science 299 (2003) 1743–1747.

- We study directional persistence in intracellular particle motion.
- We use a Hidden Markov Model to decribe active/non-active switching behavior.
- A multi-scale turning angle model describes directional persistence.
- Reference data with inhibited activation is used as calibration.
- Experiments on microtubule transport and myosin activation gives good results.